>1142<

Microstructure and superconducting properties of Yttrium barium copper oxide thin film with patterned substrates for ultra-fine multi-filaments

Akiyoshi Matsumoto, Shuuichi Ooi, Satoshi Hata, Taiki Wada, Ryo Teranishi, Yuji Tsuchiya

***Abstract*— Yttrium barium copper oxide (YBCO) superconductors are promising candidates for superconducting magnets operating at low temperatures and high magnetic fields, as well as for advanced electric power devices. Commercially available YBCO wires are manufactured in tape form, by depositing a thin YBCO layer atop multiple buffer layers on a metal substrate. This coated conductor structure closely resembles a single crystal, with well-aligned crystallographic axes, thereby exhibiting high critical current densities. However, challenges remain in reducing screening currents and AC losses for practical applications. In this study, we present a multifilamentary YBCO thin film design with patterned elevated stripes, fabricated using photolithography on substrates. Various stripe materials, including SiO_2, and Al_2O, were evaluated by depositing YBCO on the STO/stripe structures. Magnetooptical imaging demonstrated that non-superconducting stripes separate the superconducting regions, irrespective of the stripe material used. Transmission electron microscopy (TEM/STEM)-EDX analysis revealed that YBCO on STO/SiO_2 stripes formed crystals with varied orientations, whereas STO/Al_2O_3 stripes resulted in the formation of impurity phases. These findings indicate that substrate patterning with stripe structures is a viable approach for realizing multifilamentary coated conductors, potentially reducing AC losses and enhancing future superconductor applications.**

***Index Terms*— Coated conductors, Multifilamentary superconductors, Photolithography, $YBa_2Cu_3O_x$**

I. INTRODUCTION

RECENT advancements have significantly enhanced the performance and accessibility of high-temperature superconducting coated conductor (HTS-CC) tape wires, as demonstrated in numerous studies [1-5]. This progress has fueled the exploration of HTS-CC tapes for various technological applications [6-10]. However, the practical deployment of high-temperature superconductors (HTS) is constrained by the lack of multifilamentary structures and stabilization technologies, which are well established for low-temperature superconducting wires and are essential for mitigating screening currents in high-field magnet systems.

Rare-earth barium copper oxide (REBCO) CC tapes are fabricated by depositing buffer layers onto high-strength metal substrates after orientation treatment using techniques, such as ion beam-assisted deposition (IBAD) or Rolling-Assisted Biaxially Textured Substrates (RABiTS) [2,3], resulting in highly oriented thin-film structures with superior critical current densities (J_c) [11]. Nevertheless, owing to their large aspect ratio and high J_c, REBCO CC tapes are subjected to significant shielding current-induced magnetic fields and AC losses, which limit their utility in high-field magnets and power devices. Theoretical analyses have revealed that the tape geometry contributes to magnetization loss proportional to the square of the strip width [12,13]. Reducing the filament width directly reduces these losses and the accompanying hoop stress; thus, fine filamentation is highly desirable.

Multifilamentary technology, extensively used in conventional superconducting wires [14], provides an effective solution to these limitations. Recent studies have focused on minimizing the screening current effects in superconducting magnets by segmenting CC tapes using various techniques, with laser ablation scribing identified as a robust and precise method [15-20]. Approaches, such as two-level undercut profile substrates using chemical etching and polishing [18], and substrate scratching before stacking [19] have also demonstrated promise.

Note that, for magnet applications employing multifilamentary architectures, electrical insulation between filaments is not always required; reports suggest that electrical contact may enhance conductor stability [20,21], consistent with practices in Nb-Ti and Nb–Sn stabilized tapes.

Building on previous work, we developed a multifilamentary $YBa_2Cu_3O_x$ (YBCO) thin film by depositing YBCO onto substrates patterned with elevated Zr stripes via photolithography. The method of modifying this substrate to grow REBCO is referred to as a bottom-up approach, in contrast to the top-down approach where the REBCO layer is processed after deposition. The bottom-up approach allows for the deposition without damaging the REBCO layer, thereby minimizing the degradation of the critical current. This structure divides the continuous YBCO layer into discrete

Manuscript received 25 September 2025; revised 27 December 2025; accepted 12 January 2026. Date of publication ## # ###.

Akiyoshi Matsumoto and Shuuichi Ooi are with the National Institute for Materials Science, Tsukuba, Ibaraki 3050047, Japan (e-mail:matsumoto.akiyoshi@nims.go.jp).

Satoshi Hata is with the Department of Materials Science and Engineering, Kyushu University, 1-2-1 Kasuga, Fukuoka 819-0395, Japan (e-mail: teranishi@zaiko.kyushu-u.ac.jp)

Taiki Wada and Ryo Teranishi are with the Department of Materials, Kyushu University, 744 Motooka, Nishi-ku, Fukuoka 819-0395, Japan (e-mail: teranishi.ryo.438@m.kyushu-u.ac.jp).

Yuji Tsuchiya is with the Department of Applied Physics, Tohoku University, 2-1-1 Katahira Sendai, Miyagi 980-8577, Japan (e-mail: yuji.tsuchiya.c3@tohoku.ac.jp).

filaments by locally disrupting the grain orientation above the stripes, thereby suppressing intergranular current flow [22,23]. Expanding on this methodology, we investigated striped materials other than Zr, including Nb. Our study reveals that impurities, such as NbO and ZrO artificial pinning centers, examined in REBCO thin film research [24,25], have a minimal impact on J_c. However, the incorporation of Nb stripes results in distinct impurity phases that inhibit YBCO crystallization on Nb due to unfavorable chemical interactions, as confirmed by detailed transmission electron microscopy (TEM)/ scanning transmission electron microscopy (STEM) analyses. This underscores the critical importance of the stripe material selection in optimizing the microstructural and superconducting properties of multifilamentary HTS-CC architectures.

II. Experimental

Photolithography, a versatile technique widely applied in semiconductor device fabrication, was employed to produce multicore thin-film superconducting wires [22,23]. Initially, a resist solution was spin-coated onto an STO substrate, followed by pattern definition and development using a maskless exposure system. After development, grooves were formed in the resist layer, and Al_2O_3 or SiO_2 was deposited into these grooves by sputtering. The subsequent lift-off removal of the resist resulted in the formation of line-shaped oxide protrusions. Table 1 shows specification of one stripe line of each oxide materials. The YBCO thin film was then deposited onto the patterned STO substrate by pulsed laser deposition (PLD) using a KrF excimer laser and YBCO target.

The microstructural characterization of the samples was performed using several advanced techniques. Magneto-optical (MO) imaging was used to evaluate the superconductivity of the patterned films. Scanning electron microscopy (SEM, Hitachi High-Tech SU-70) was used for detailed surface observations. TEM and STEM were performed using a JEOL-ARM system to investigate the microstructure in the vicinity of the striped regions. STEM-EDS observations were performed using a Titan Cubed G2 electron microscope (Thermo Fisher Scientific) at an acceleration voltage of 300 kV. The specimens for the STEM-EDS observations were prepared using a focused ion beam mill (Scios, Thermo Fisher Scientific).

Table 1 Specification of stripe structure on STO substrates and process condition of PLD deposition.

Stripe material	Al_2O_3	SiO_2
Sputtering time (sec.)	2400	1200
Width after lift-off (μm)	3.4	2.8
Hight after lift-off (nm)	85	44
PLD energy (mJ)	100	
PLD reputation (Hz)	10	
Substrate temperature (K)	1033	
Deposition time(min.)	60	
Atmosphere	100 mTorr O_2	

III. Results and Discussion

Fig. 1 shows the results of MO imaging for stripe patterns fabricated using (a) Al_2O_3 and (b) SiO_2 stripes. The white regions in the images correspond to areas where magnetic flux penetration occurs at 50 K, indicating the presence of nonsuperconducting regions at this temperature. These images demonstrate that both superconducting and nonsuperconducting layers were formed in accordance with the designed patterns. Note that partial truncation is observed at the edges of some samples due to localized resist accumulation during the patterning process. Despite the use of different pattern designs for the SiO_2 and Al_2O_3 stripes, the separation between superconducting and non-superconducting regions follows the patterns defined before YBCO film deposition.

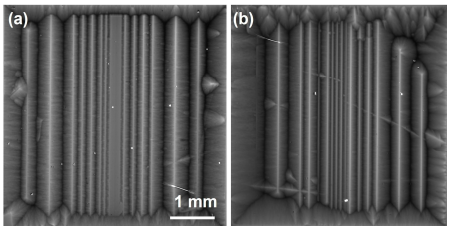

Fig. 1. (a) Al_2O_3-stripes MO images at 42 mT with the magnetic field increasing up to 42 mT before decreasing to 0 mT at 50 K. (b) SiO_2 stripes.

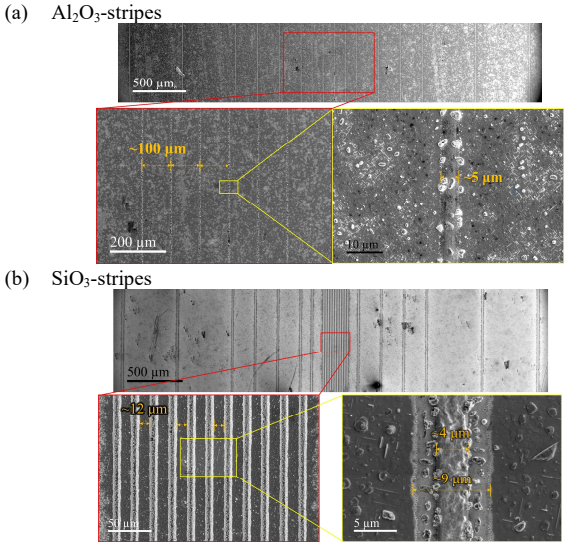

Fig. 2. SEM images of surface of (a)Al_2O_3 stripe and SiO_2 stripes. Images were captured at different magnifications around the stripes.

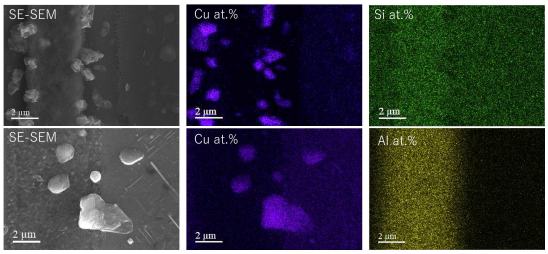

Fig. 3. Laser microscope images after making Nb-stripes. The measurement results below indicate the height measurements of the area indicated by the upper line.

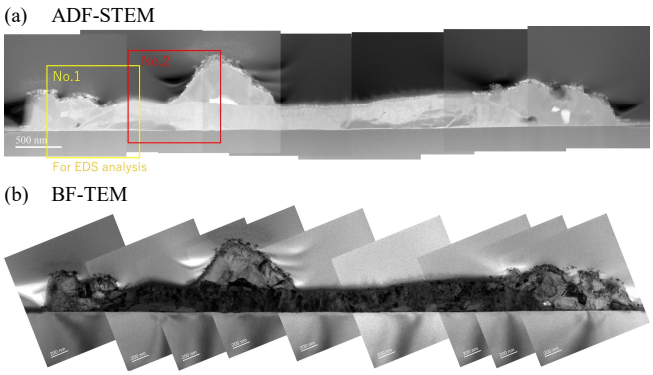

Fig. 4. STEM images (a) ADF-STEM and (b) BF-STEM of the cross-section of the area near the edge of SiO_2 strip.

Fig. 2 shows SEM images of the sample surfaces at various magnifications, highlighting both the overall morphology and localized regions of interest. Low-magnification images reveal distinct microstructures within the stripe areas of both SiO_2 and Al_2O_3 samples, which differ noticeably from those of the surrounding matrix. The intended width of the stripe structures for both SiO_2 and Al_2O_3 was 5 µm. On SiO_2, while the stripe itself measures approximately 5 µm, additional regions with unique microstructural characteristics—each approximately 3 µm wide—are observed on both sides of the stripe, differing from the matrix. In contrast, the Al_2O_3 stripes remain well confined to the designed 5 µm width, with no significant formation of adjacent regions, indicating improved fidelity in pattern transfer for the Al_2O_3 stripes.

Fig. 3 shows the elemental mapping of each thin-film sample obtained through EDX analysis. The EDX results revealed that the regions exhibiting pronounced charging and appearing bright in the SEM images correspond to areas with Cu-rich concentrations, indicating the local formation of CuO. Further mapping of Si and Al, the materials used in stripe patterning, demonstrates distinct behaviors: Si is distributed not only within the stripe features but also across the surrounding regions, whereas Al is primarily localized within the designed stripe structures. These results highlight the differences in elemental dispersion associated with the patterning process.

Fig. 4 shows STEM images acquired from the Si stripe region, which was prepared by micro-sampling. The annular dark-field (ADF) and high-angle annular dark-field (HAADF) images indicate that both ends of the sampled region were devoid of material, corresponding to the gray areas adjacent to the stripes observed in the SEM images shown in Fig. 2. These observations confirm that YBCO was not formed in the regions adjacent to the stripe owing to chemical interactions with Si.

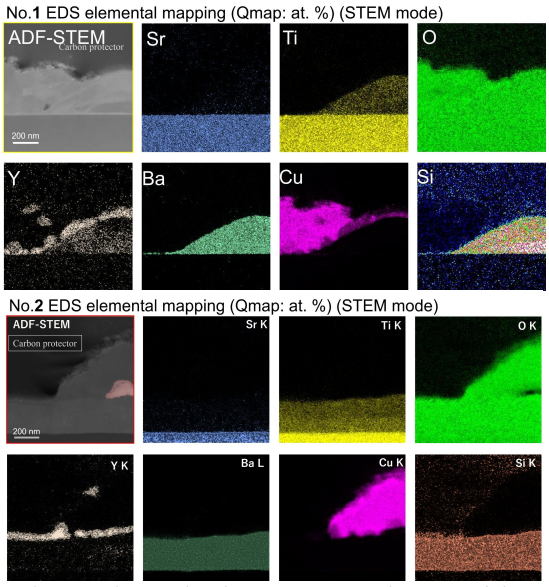

Fig.5. Elemental mapping by STEM-EDS images of the cross-section of the area near the middle of the SiO_2 stripe(No. 1 and 2 from Fig. 4).

The transmission electron microscopy energy-dispersive X-ray spectroscopy (STEM-EDS) results are shown in Fig. 5. Elemental analysis of Regions 1 and 2 revealed pronounced Cu

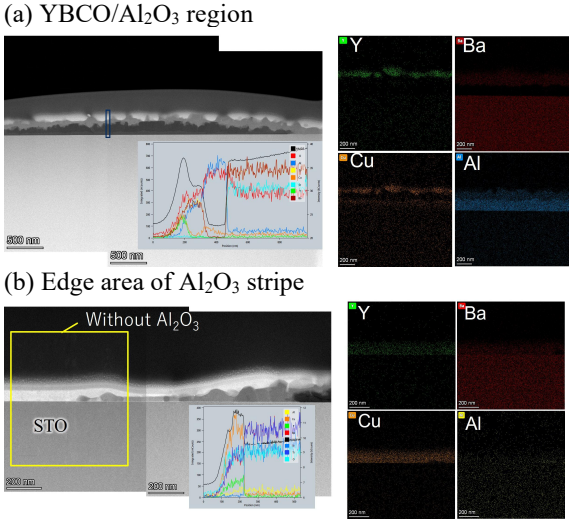

Fig. 6. HAADF-STEM images of the cross section of the area near the Al_2O_3 strip. (a)YBCO/Al_2O_3 region and (b)edge area of Al_2O_3 stripe. The images on the right show elemental maps of Y, Ba, Cu and Al. Insets display line profiles of each position.

enrichment, coinciding with areas where neither Y nor Ba were present, indicating localized CuO formation. Conversely, Ba and Si are detected at nearly equal concentrations, suggesting the formation of Ba_2Si based on the Ba–Si phase diagram[26]. Despite the high melting point of Si, the eutectic reaction between Ba and Si facilitates the formation of Ba_2Si at temperatures below 800 °C. Given that the substrate temperature during deposition was approximately 700°C, these results imply that Ba introduced via pulsed laser deposition (PLD) preferentially reacts with Si to form Ba_2Si. This process

inhibits the formation of YBCO in regions containing Si, providing insights into the chemical interactions governing the film microstructure.

Fig. 6 present cross-sectional STEM images and corresponding elemental line analyses of regions adjacent to the Al_2O_3 stripes. Fig. 6(a) focuses on the area directly atop the stripe, whereas Fig. 6(b) examines a region slightly offset from the stripe. Elemental mapping performed by EDX indicates that Al is localized exclusively within the Al_2O_3 stripes on the stripe and is scarcely detected in the adjacent matrix (Fig. 6(b)). These observations confirm that Al_2O_3 remains precisely in its patterned location after stripe fabrication, without exhibiting any measurable diffusion. Moreover, Al_2O_3 is chemically inert with respect to Y, Ba, and Cu, in contrast to Si, which forms reaction layers that extend beyond the intended stripe region and disrupt the YBCO film. The use of an insulating material that does not react with Y-Ba-Cu offers the potential to reduce hysteresis losses, thereby decreasing AC losses in superconducting applications. However, the formation of a reaction layer in Si-based patterns could diminish the effective current-carrying capability by damaging the YBCO layer beyond the design specifications. Further electrical resistivity measurements and compositional studies will be necessary to identify the most suitable insulating materials for these applications. Furthermore, in practical applications, it is necessary to fabricate structures suitable for each specific application, and it will be essential to investigate the dependencies on various shapes in the future.

IV. Conclusion

In this study, we fabricated a YBCO film by depositing strip-shaped nonaligned metals SiO_2 and Al_2O_3 on an STO substrate using photolithography. Based on the MO images and microstructural observations, the YBCO regions were distinguishable because of the nonsuperconducting phases of SiO_2 and Al_2O_3. A detailed microstructural analysis showed that both Si and Al can form non-superconducting regions. Notably, Si reacted with YBCO, resulting in the formation of a reaction zone that extended significantly beyond the initially designated area. In contrast, Al exhibits only minimal lateral diffusion at the stripe edges, resulting in negligible effects on the superconducting phase. Due to its intrinsic insulating properties, as opposed to metallic materials, Al_2O_3 holds considerable promise as a stripe material for achieving well-confined non-superconducting regions without adverse impacts on the overall performance of superconducting films.

V. Acknowledgement

We thank Dr. Zimeng Guo, Hongye Gao, and Haosan Shi of Kyushu University for supporting the STEM observations. Part of this study was supported by the "Advanced Research Infrastructure for Materials and Nanotechnology in Japan (ARIM)" of the Ministry of Education, Culture, Sports, Science, and Technology (MEXT).

References

[1] C. Senatore, C. Barth, M. Bonura, M. Kulich and G. Mondonico, “Field and temperature scaling of the critical current density in commercial REBCO coated conductors”, Supercond. Sci. Technol. 29(2015), 014002.

[2] Y. Iijima, N. Tanabe, O. Kohno, and Y keno, “In-plane aligned $YBa_2Cu_3O_{7-x}$ thin films deposited on polycrystalline metallic substrates Appl. Phys. Lett. 60(1992), 769.

[3] A. Goyal, D. P. Norton, J. D. Budai, M. Paranthaman, E. D. Specht, D. M. Kroeger, D. K. Christen, Q. He, B affian, F. A. List, D. F. Lee, P. M. Martin, C. E. Klabunde, E. Hartfield, and V. K. Sikka, High critical current density superconducting tapes by epitaxial deposition of $YBa_2Cu_3O_x$ thick films on biaxially textured metals. Appl. Phys. Lett. 69,(1996) 1795

[4] D. Uglietti, A review of commercial high temperature superconducting materials for karge scale magnets: from wiews and tapes to cables and conductors, Supercond. Sci. Technol. 32(2019), 053001

[5] W. Prusseit, M. Bauer, V. Große, R. Semerad, G. Sigl, M. Dürrschnabel, Z. Aabdin and O. Eibl, Working around HTS thickness limitations-towards 1000+A cm-1 -Class Coated Conductors, Phys. Proc. 36(2012), 1417–22

[6] M. Iwakuma, H. Hayashi, H. Okamoto, A. Tomioka, M. Konno, T. Saito, Y. Iijima, Y. Suzuki, S. Yoshida, Y. Yamada, T. Izumi, Y. Shiohara, Development of REBCO superconducting power transformers in Japan, Physica C. 469(2009), 1726.

[7] W. D. Markiewicz, D. C. Larbalestier, H. W. Weijers, A. J. Voran, K. W. Pickard, W. R. Sheppard, J. Jaroszynski, A. Xu, J. Lu, A. V. Gavrilin, P. D. Noyes, Design of a Superconducting 32 T Magnet with REBCO High Field Coils, IEEE Trans. Appl. Supercond. 22(2012), 4300704

[8] J. Bascunan, S. Hahn, D. K. Park, Y. Kim, Y. Iwasa, On the 600 MHz HTS Insert for a 1.3 GHz NMR Magnet, IEEE Trans. Appl. Supercond. 22(2012), 4302104

[9] L. Rossi, A. Badel, M. Bajko, A. Ballarino, L. Bottura, M. M. J. Dhallé, M. Durante, Ph. Fazillea, J. Fleiter, W. Goldacker, E. Härö, A. Kario, G. Kirby, C. Lorin, J. van Nugteren, G. de Rijk, T. Salmi, C. Senatore, A. Stenvall, P. Tixador, A. Usoskin, G. Volpini, Y. Yang, N. Zangenberg, The EuCARD-2 Future Magnets European Collaboration for Accelerator-Quality HTS Magnets, IEEE Trans. Appl. Supercond. 25(2015), 4001007

[10] P. V. Gade, C. Barth, C. Bayer, W. H. Fietz, F. Franza, R. Heller, K. Hesch, K.-P. Weiss, Conceptual Design of a Toroidal Field Coil for a Fusion Power Plant Using High Temperature Superconductors, IEEE Trans. Appl. Supercond. 24(2014), 4202705

[11] D. Dimos, P. Chaudhari, J. Mannhart, and F. K. LeGoues, Orientation Dependence of Grain-Boundary Critical Currents in YBa2Cu3O7-δ Bicrystals, Phys. Rev. Lett. 61(1988), 219.

[12] E. H. Brandt and M. Indenbom, Type-II-superconductor strip with current in a perpendicular magnetic field, Phys. Rev. B 48(1993) 12893.

[13] E Zedov, J. R. Clem, M. McElfresh and M. Darwin, Magnetization and transport currents ithin superconducting films, Phys. Rev. B 49(1994) 9802.

[14] F. Grilli, A. Kario, How filaments can reduce AC losses in HTS coated conductors: a review, Supercond. Sci. Technol. 29(2016), 083002

[15] S. Terzieva, M. Vojenciak, F. Grilli, R. Nast, J. Souc, W. Goldacker, A. Jung, A. Kudymow, A. Kling, Investigation of the effect of striated strands on the AC losses of 2G Roebel cables Supercond. Sci. Tecnol. 24 (2011), 045001

[16] M. D. Sumption, E. W. Collings, P. N. Barnes, AC loss in striped (filamentary) YBCO coated conductors leading to designs for high frequencies and field-sweep amplitudes. Supercond. Sci. Technol. 18 (2005), 122

[17] T. Machi, K. Nakao, T. Kato, T. Hirayama, K. Tanabe, Reliable fabrication process for long-length multi-filamentary coated conductors by a laser scribing method for reduction of AC loss Supercond. Sci. Tecnol. 26 (2013), 105016

[18] A. C. Wulff, M. Solovyov, F. Gomory, A. B. Abrahamsen, O. V. Mishin, A. Usoskin, A. Rutt, J. H. Lundeman, K. Thyden, J. B. Hansen, J.-C. Grivel, Two level undercut-profile substrate for filamentary YBa2Cu3O7 coated conductors Supercond. Sci. Technol. 28 (2015), 072001

[19] S. Fujita, S. Muto, C. Kurihara, H. Sato, W. Hirata, N. Nakamura, M. Igarashi, S. Hanyu, M. Daibo, Y. Iijima, K. Naoe, M. Iwakuma, T. Kiss, Characterization of Multifilamentary REBCO Coated Conductor Coil Fabricated by Using the Process of Scratching the IBAD-MgO Layer. IEEE Trans. Appl. Supercond. 27 (2017), 6600504.

[20] Y. Sogabe, Y. Mizobata, and N. Amemiya, “Coupling time constants and ac loss characteristics of spiral copper-plated striated coatedconductor cables (SCSC cables),” *Supercond. Sci. Technol.,* vol. 33, 2020, Art. no. 055008.

[21] N. Amemiya et al., “Effective reduction of magnetization losses in copperplated multifilament coated conductors using spiral geometry,” *Supercond. Sci. Technol.,* vol. 35, 2022, Art. no. 025003.
[22] A. Matsumoto, M. Tachiki, S. Ooi, Development of YBCO patterned Multi-Filamentary Film Using Photolithography Method, IEEE Trans. Appl. Supercond. 33(2023), 7500404.
[23] A. Matsumoto, M. Tachiki, S. Ooi, R. Teranishi, M. Inoue, Microstructural study of YBCO thin films with stripe-pattered substrates for ultra-fine multi-filaments, IEEE Trans. Appl. Supercond. 34(2024), 7500404.
[24] J. L. MacManus-Driscoll, S. R. Foltyn, Q. X. Jia, H. Wang, A. Serquis, L. Civale, B. Maiorov, M. E. Hawley, M. P. Maley & D. E. Peterson, Strongly enhanced current densities in superconducting coated conductors of YBa2Cu3O7–x + BaZrO3, Nat. Mat. 3(2004), 439.
[25] S. H. Wee, A. Goyal, Y. L. Zuev, C. Cantoni, V. Selvamanickam and E. D. Specht, Formation of Self-Assembled, Double-Perovskite, Ba_2YNbO_6 Nanocolumns and Their Contribution to Flux-Pinning and J_c in Nb-Doped $YBa_2Cu_3O_{7-\delta}$ Films, Appl. Phys. Express 3(2010) 023101.
[26] M. Pani, A. Palenzona, The phase diagram of the Ba-Si system, Journal of Alloys and Comp. 454 (2008), L1.